DOI: 10.1002/asia.200600042

Mono- and Di(dimethylamino)styryl-Substituted Borondipyrromethene and Borondiindomethene Dyes with Intense Near-Infrared Fluorescence

Yan-Hong Yu,[a] Ana B. Descalzo,[b] Zhen Shen,*[a] Holger Röhr,[b] Quan Liu,[a] Yan-Wei Wang,[a] Monika Spieles,[b] Yi-Zhi Li,[a] Knut Rurack,*[b] and Xiao-Zeng You*[a]

Abstract: Four novel borondipyrromethene (BDP) and -diindomethene (BDI) dyes with one or two (dimethylamino)styryl extensions at the chromophore were synthesized and spectroscopically investigated. An X-ray crystal structure shows that the extended auxochrome is virtually planar. All dyes thus display intense red/near infrared (NIR) absorption and emission. The (dimethylamino)styryl group induces a charge-transfer character that entails bright solvatochromic fluorescence, which is only quenched with increasing solvent polarity according to the energy-gap law. The dye with an additional dimethylanilino group at the *meso* position of BDP shows a remarkable switching of lipophilicity by protonation. Two dyes with an 8-hydroxyquinoline ligand at the *meso* position display quenched emission in the presence of Hg^{2+} or Al^{3+} owing to electron transfer from the excited BDP to the complexed receptor. The BDI dye presents a pH indicator with bright fluorescence and extremely low fluorescence anisotropy.

Keywords: borondipyrromethene · dyes · fluorescence · indicators · protonation

Introduction

The development of functional dyes that absorb and emit in the red visible or near-infrared (NIR) region of the optical spectrum has received increasing attention in the last decade. Although there has been considerable interest in NIR dyes since the early/middle of the last century,[1] from advances in photography[2] through attempts at optical data storage[3] and lasing[4] to novel low-noise detection techniques in various analytical methods such as electrophoresis[5] or immunoassays,[6] research in this area showed a real boost only with the technological advances in NIR imaging instrumentation. Thus, nowadays NIR dyes play a prominent role in many fields of medicinal chemistry and biotechnology, ranging from tomography[7] through endoscopic imaging[8] and tumor diagnostics[9] to drug discovery[10] and nucleic acid detection.[11] Traditionally, cyanine dyes such as Cy3 or Cy5 are the most widely used chromophores in these applications (Scheme 1). However, whereas their absorption characteristics are very favorable (high molar absorptivities),[1] their fluorescence quantum yields often do not exceed moderate values (5–15%). This is basically due to the flexible (poly)methine chain between the two terminal moieties that allows photoisomerization in the excited state to a substantial degree.[12] The synthesis of more-rigid cyanines, however, is synthetically demanding[13] and such dyes occupy only a niche in the above-mentioned applications.

As a promising alternative, borondipyrromethene (BDP) derivatives have gained strong popularity in these fields (Scheme 1). BDP dyes can be seen as rigid, cross-conjugated cyanines (see below) and the majority of BDPs have been developed to complement or substitute classic fluorophores such as fluorescein and certain rhodamines, that is, fluorophores of the visible range.[14] Accordingly, many different examples of BDPs as fluorescent probes, labels, or indicators have been reported recently.[15,16] BDPs are also frequently used as building blocks in molecular optoelectronic devices,

[a] Y.-H. Yu, Prof. Z. Shen, Q. Liu, Y.-W. Wang, Prof. Y.-Z. Li, Prof. X.-Z. You
Coordination Chemistry Institute, State Key Laboratory of Coordination Chemistry, School of Chemistry and Chemical Engineering, Nanjing University
Nanjing, 210093 (China)
Fax: (+86) 25-8331-4502
E-mail: zshen@nju.edu.cn
youxz@nju.edu.cn

[b] Dr. A. B. Descalzo, H. Röhr,[+] M. Spieles, Dr. K. Rurack
Div. I.5, Bundesanstalt für Materialforschung und -prüfung (BAM)
Richard Willstätter Strasse 11, 12489 Berlin (Germany)
Fax: (+49) 30-8104-5005
E-mail: knut.rurack@bam.de

[+] Associated with: Fachbereich Biologie, Chemie, Pharmazie
Freie Universität Berlin, Takustrasse 3, 14195 Berlin (Germany)

Supporting information for this article is available on the WWW under http://www.chemasianj.org or from the author.

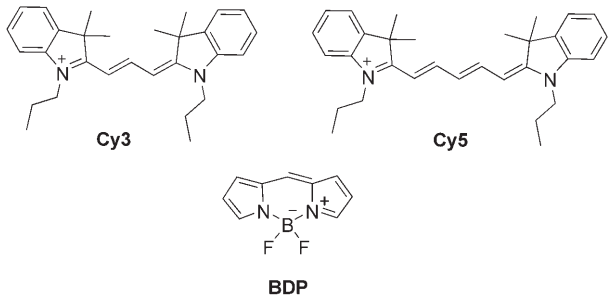

Scheme 1. Chemical structures of the popular cyanine labels Cy3 and Cy5 and the BDP core.

energy-transfer cascades, or multimode switches.[17,18] The simple BDP core absorbs and emits in the 480–540-nm region. As the BDP core principally combines the advantageous cyanine properties of high molar absorptivity and narrow band shapes with high fluorescence yields (typically >50%), various research groups have strived to obtain BDP derivatives for the wavelength range beyond 600 nm.[19–22] On the basis of our efforts in this direction,[20–22] we present herein the synthesis and characteristics of the newly designed borondipyrromethene (BDP) and borondiindomethene (BDI) dyes **1**–**4**, for which the chromophoric π system is elongated by either one or two (dimethylamino)styryl groups (Scheme 2). Dyes **1**–**4** are further equipped with different functional groups in the *meso* position, hence allowing us not only to study the spectroscopic characteristics of the chromophoric cores themselves but also to obtain additional insight into selected aspects of signaling chemistry. The dyes collected in Scheme 3 were employed as model compounds at various stages of the work.

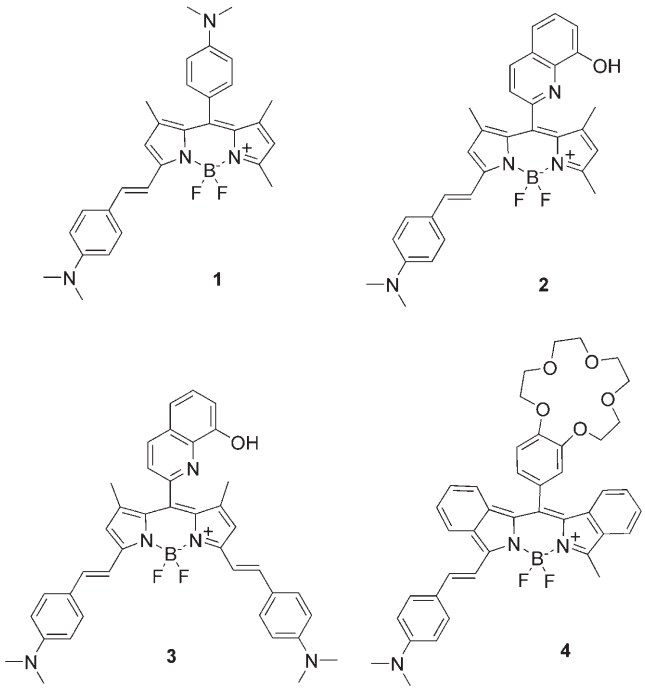

Scheme 2. Long-wave absorbing and emitting dyes studied in this work.

Results and Discussion

Synthesis

Compounds **1**–**4** were prepared by condensation of 4-dimethylaminobenzaldehyde with borondipyrromethenes **6**,[18] **7**,[23] or **10**[20] (Scheme 3), in the presence of piperidinium acetate as a catalyst.[21] Interestingly, condensation of 4-dimethylaminobenzaldehyde with **7** gave products **2** and **3** simultaneously. After short reaction times (e.g. 15 h) the asymmetric compound **2** was separated as the main product; when the reaction time was extended to 1 week, compound **3** was dominant. Notably, under reflux conditions the bicyclo[2.2.2]octadiene group in **10** was converted into a benzene ring through a retro-Diels–Alder reaction and gave conjugated compound **4** as the primary product.

Abstract in Chinese:

基于近红外材料在信息和传感科学中的应用，设计合成了四个新型的外接一个或两个（二甲基氨基）苯乙烯基助色团的硼-二吡咯亚甲基(BDP)和硼-二吲哚亚甲基(BDI)荧光染料，研究了它们的光谱性质。对其中一个分子的X-射线结构分析表明，其外接的助色团几乎是平面性的。所有的染料分子在红光/近红外区域都显示出很强的吸收和发射光谱。根据能隙定律，（二甲基氨基）苯乙烯基诱导的电荷转移使得溶剂化显色荧光随着溶剂的极性增强而被淬灭。在BDP的中位连接了另一个二甲基氨基基团的染料分子显示了显著的质子化作用诱导的亲脂性转换。中位连接了8-羟基喹啉的配体在汞离子或铝离子存在下，其荧光被淬灭。这是由于电子从激发态的BDP染料转移到了配位的受体上。BDI染料显示出强的荧光和极低的荧光各向异性，可望作为一种pH指示剂。

Crystal Structure of 1

Cell parameters and refinement details for compound **1** are summarized in Table 1. Figure 1 shows a perspective view of the molecular conformation of **1**. The average bond lengths for B–N and B–F and the average N–B–N and F–B–F angles indicate a tetrahedral BF_2N_2 configuration and are in good agreement with previously published data.[20,24] The bond length C16–C17 is 1.332(3) Å, indicating a double bond in the *trans* conformation. The C10–C15 aryl ring is virtually perpendicular to the indacene plane (dihedral angle of 82.5°). The C18–C23 aryl ring and the C16=C17 bond are essentially coplanar (dihedral angle is 0.67°). The styryl group is also only slightly twisted by 5° out of the plane of the main BDP core, suggesting efficient conjugation within the entire chromophore. The nitrogen atoms of both dimethylamino groups show only negligible pyramidalization, and the sum of the dihedral angles at N3 and N4 is 354°. The lone pairs of electrons are thus in conjugation with the short N3–C13 and N4–C21 bonds (average value:

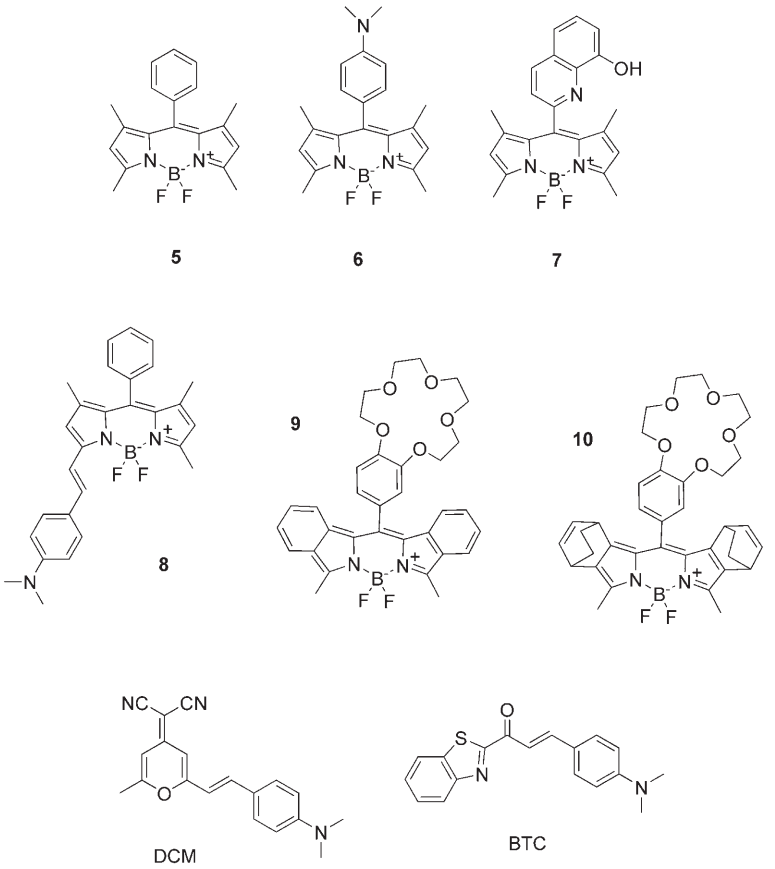

Scheme 3. Model compounds used in the work.

Table 1. Crystallographic data and structure refinement for **1**.

Formula	$C_{30}H_{33}BF_2N_4$
FW	498.41
T [K]	293 (2)
Crystal system	Monoclinic
Space group	$P21/c$
a [Å]	19.299(4)
b [Å]	6.5714(14)
c [Å]	21.040(5)
α [°]	90
β [°]	97.179(5)
γ [°]	90
V [Å^3]	2647.4(10)
Z	4
ρ_{calcd} [g cm^{-3}]	1.250
F (000)	1056
Crystal size [mm]	0.24 × 0.26 × 0.30
μ [cm^{-1}]	0.084
λ [Å]	0.71073
$2\theta_{max}$ [°]	26.0
Reflections collected	5173
Reflections observed/[$I>2\sigma$ (I)]	3258
Parameters	339
R1 (on F) [$I>2\sigma$ (I)]	0.043
wR (all)	0.1301
Goodness of fit	0.991
Largest difference peak and hole [eÅ^{-3}]	0.17 and −0.20

1.322(3) Å) of the aryl and styryl groups, respectively. There are no π–π stacking interactions between the asymmetrical molecules in compound **1**.

Absorption and Fluorescence Spectroscopy of 1–4

To gain insight into their photophysical properties, the red and NIR emitting dyes **1–4** were investigated by absorption as well as steady-state and time-resolved fluorescence spectroscopy in a variety of solvents of different polarity (Table 2). The solvatochromism and/or solvatokinetics of model compounds **5**, **6**, **8**, and **9** were previously studied by us,[20,21,25] and the relevant data are included in the Supporting Information for a better comparison. The spectroscopic properties of the other model compounds have been determined in selected solvents and for specific comparisons.

The absorption maxima of the mono(dimethylamino)styryl-substituted BDPs **1** and **2** are centered at approximately 600 nm, about 100 nm further to the red than simple BDP dyes such as **5**, and show only a

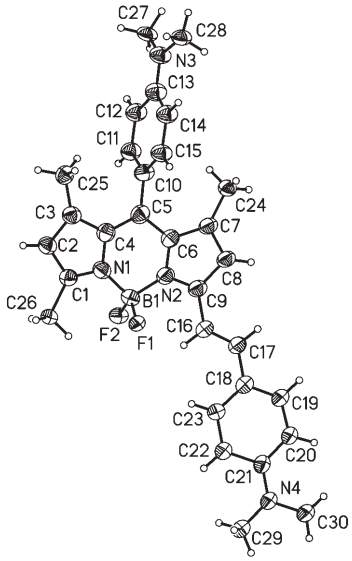

Figure 1. ORTEP plot of **1** with thermal ellipsoids drawn at the 30% probability level. Selected bond lengths (Å) and angles (°): F1–B1 1.356(3), F2–B1 1.351(3), N1–B1 1.471(3), N2–B1 1.483(4), N1–C1 1.266(3), N2–C9 1.284(3), N1–C4 1.348(3), N2–C6 1.338(3), C16–C17 1.332(3); N1–B1–N2 106.4(2), F1–B1–F2 108.9(2).

Table 2. Spectroscopic and photophysical properties of **1**–**4** in various solvents at 298 K.

	Solvent	λ_{abs} [nm]	log ε_{max}	λ_{em} [nm]	$\Delta\tilde{\nu}_{abs-em}$ [cm^{-1}]	Φ_f	τ_f [ns]	k_r [$10^8\ s^{-1}$]	k_{nr} [$10^8\ s^{-1}$]
1	MeOH	594	4.83	699	2700	0.10	0.62	1.6	14.5
	MeCN	595	4.84	719	3080	0.05	0.33	1.5	28.8
	CH_2Cl_2	601	4.89	672	1920	0.68	3.40	2.0	0.9
	THF	597	4.95	661	1810	0.65	3.22	2.0	1.1
	Et_2O	591	4.96	632	1270	0.78	3.62	2.2	0.6
	Bu_2O	593	4.98	623	850	0.84	3.67	2.3	0.4
	hexane	590	n.d.[a]	604	380	0.78	3.56	2.2	0.6
2	MeOH	608	4.77	738	3100	0.04	0.27	1.5	35.6
	MeCN	609	4.79	758	3420	0.05	0.33	1.4	28.9
	CH_2Cl_2	618	4.79	711	2240	0.45	2.61	1.7	2.1
	THF	612	4.83	700	2190	0.43	2.42	1.8	2.4
	Et_2O	605	4.88	666	1640	0.52	2.93	1.8	1.6
	Bu_2O	608	4.89	650	1150	0.64	2.95	2.2	1.2
	hexane	606	n.d.[a]	627	600	0.28	1.50	1.9	4.8
3	MeOH	705	4.82	791	1640	0.07	0.60	1.2	15.4
	MeCN	711	4.82	807	1690	0.10	0.83	1.2	10.9
	CH_2Cl_2	718	4.86	784	1240	0.29	1.58	1.8	4.5
	THF	709	4.93	762	1040	0.29	1.62	1.8	4.4
	Et_2O	697	4.97	736	810	0.36	2.20	1.6	2.9
	Bu_2O	699	4.96	732	650	0.50	2.38	2.1	2.1
	hexane	693	n.d.[a]	712	410	0.45	2.68	1.7	2.1
4	MeOH	691	4.85	732	850	0.20	1.63	1.2	4.9
	MeCN	693	4.84	741	980	0.24	2.20	1.1	3.5
	CHon	703	4.89	739	740	0.28	2.20	1.3	3.3
	THF	697	4.90	726	620	0.30	2.37	1.3	2.9
	Et_2O	688	4.97	709	480	0.39	2.81	1.4	2.2
	Bu_2O	690	4.96	709	410	0.45	2.88	1.6	1.9
	hexane	685	n.d.[a]	697	250	0.35	3.30	1.1	2.0

[a] Not determined due to low solubility. THF = tetrahydrofuran, CHon = cyclohexanone.

slight red shift with increasing solvent polarity (Figure 2). Similar features have been found for the BDI chromophore. For instance, **4** absorbs at 689 nm in diethyl ether, whereas the band maximum of **9** is found at 598 nm in that solvent. Upon introduction of the second (dimethylamino)styryl arm from **2** to **3**, the absorption maxima are further displaced by about 100 nm to the red (Figures 2 and 3). Besides these spectral characteristics, a broadening of the lowest-energy absorption band as a function of solvent polarity is noticed for **1**–**4** (Figures 2 and 3). For instance, the width at half maximum (fwhm) increases from 960/1010/910/960 cm^{-1} to 1780/1950/1710/1500 cm^{-1} for **1**–**4** upon going from hexane to acetonitrile. However, regardless of solvent polarity and spectral broadening, the polymethine nature of the BDP and BDI chromophores is manifested in the molecular C–C frame vibration of about 1300 cm^{-1} that is typical for cyanine dyes.[26] Furthermore, although the width of the spectrum increases with solvent polarity, the concomitant reduction in molar absorptivity (Table 2) leads to virtually unchanged integrals of the lowest-energy absorption bands or oscillator strengths. The nature of the states involved in the absorption process thus does not change with solvent polarity. The bathochromic shifts mentioned above are reminiscent of the "vinylene shift" of polymethine dyes[12] and indicate the extension of the auxochrome. The generally preserved shape and the polarity-induced broadening further suggest that charge-transfer character is admixed to the polymethine nature.

Whereas the shifts in absorption are on the order of ±5 nm, the fluorescence bands show a more pronounced solvatochromism, entailing differences between hexane and acetonitrile $\Delta\tilde{\nu}^{em}_{max}$(hex–MeCN) of about 2850 cm^{-1} for **1** and **2**, 1650 cm^{-1} for **3**, and 920 cm^{-1} for **4**. At the same time, the Stokes shift increases for all the dyes with solvent polarity (Table 2). Figure 2 shows that, especially for **1** and

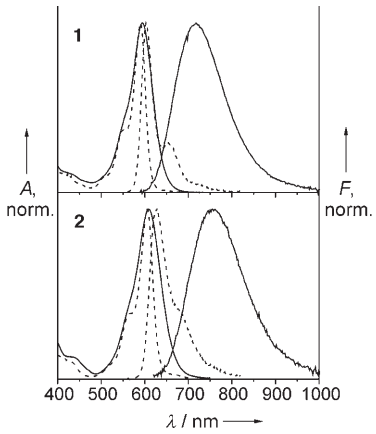

Figure 2. Absorption (*A*) and fluorescence (*F*) spectra of **1** (top) and **2** (bottom) in acetonitrile (——) and hexane (-----) at 298 K.

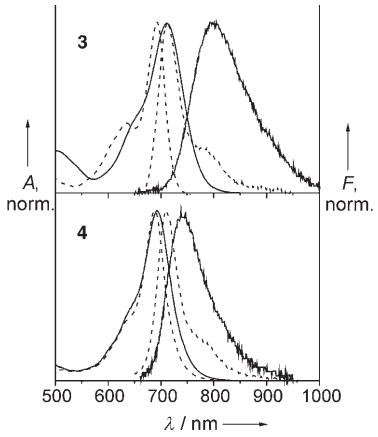

Figure 3. Absorption (*A*) and fluorescence (*F*) spectra of **3** (top) in acetonitrile (——) and hexane (-----) and **4** (bottom) in acetonitrile (——) and diethyl ether (-----) at 298 K.

2, the typical mirror-image relationship of BDP absorption and emission is lost as a function of solvent polarity. In accordance with our recent findings on **8**,[21] these observations can be attributed to the activation of an excited-state intramolecular charge-transfer (ICT) process. However, the ICT in the title dyes is rather moderate when compared to those of the related merocyanine or styryl dyes such as DCM or BTC (Scheme 3), which have a strong ICT character ($\Delta\tilde{\nu}^{em}_{max}$(hex−MeCN) = 4350 and 6070 cm^{-1}, respectively). Consequently, application of the Lippert–Mataga[27] formalism to a correlation of Stokes shift versus solvent polarity function $f(\varepsilon)-f(n^2)$ yields a change in dipole moment of 16.5, 16.9, 11.4, and 9.3 D for **1**–**4**,[28] respectively, which is considerably smaller than those found for the classic ICT dyes BTC (19.7 D)[29] and DCM (20.2 D).[30] Moreover, the second dimethylamino group in **3** does not increase the ICT character, but the step from an asymmetric to a symmetric π system reinforces the polymethine character.

The fluorescence quantum yields of **1**–**4** in medium and nonpolar solvents are considerably high; those of the NIR-emitting dyes **3** and **4** are lower than those of **1** and **2** (Table 2). Furthermore, the fluorescence yield for **1** and **2** decreases about tenfold upon changing from dichloromethane to acetonitrile. For **3**, this effect is less pronounced, and is almost absent for **4**. These trends are reflected by the rates of nonradiative decay, $k_{nr}=(1-\Phi_f)/\tau_f$: a change from dibutyl ether to acetonitrile leads to a two- and fivefold increase for **4** and **3**, yet 24- and 72-fold for **2** and **1** (Table 2). The table also reveals that the radiative rate constants, $k_r=\Phi_f/\tau_f$, decrease slightly for all the dyes when the emission band maximum undergoes a red shift. The latter can be explained by the dependence of k_r on the emission band position, and the reduced radiative rate constants κ_f differ only statistically for **1**–**4** in the solvents studied.[31] The nature of the emitting state thus does not change upon altering solvent polarity, suggesting that an emitting ICT state is directly populated after initial relaxation of the Franck–Condon state and no other emitting states play a major role.

Analysis of the dependence of k_{nr} on the emission energy provides information on the solvatokinetic features. According to the energy gap law,[32] the rate constant of internal conversion k_{ic} is enhanced as the energy gap between the ground and first excited singlet state decreases. Figure 4 shows such a plot for **1** and **4** as an example, and similar results were obtained for **2** and **3** in medium and nonpolar solvents. From these correlations it is evident that the positive solvatokinetic behavior of **3** and **4** is due to enhanced internal conversion. In **1** and **2**, a further process leads to the jump in k_{nr} upon changing from CH_2Cl_2 to MeCN and MeOH. On the basis of the similarity of the spectral features of model compounds **8** and **1** (Table 2 and Table S1 in the Supporting Information), the behavior of **1** in highly polar solvents can be ascribed to the activation of a competitive non-emitting process, most probably a second charge transfer (CT_2) (Scheme 4). Owing to the perpendicular arrangement of the *meso* donor and the BDP core acceptor, this CT_2 is largely forbidden and hence proceeds through a nonradiative pathway.[20,33] The driving force for this process can be calculated from the photophysical parameters of **1** and **8** under the assumption that no other process is involved in the radiationless deactivation according to $k=(\tau_f)^{-1}-(\tau_f^{ref})^{-1}$ ($(\tau_f)^{-1}$ and $(\tau_f^{ref})^{-1}$ are the reciprocal fluorescence lifetimes of quenched **1** and unquenched model **8**, respectively). With $(\tau_f^{ref})^{-1}=10.6\times10^8\ s^{-1}$ and $(\tau_f)^{-1}=30.3\times10^8\ s^{-1}$, $k=2\ ns^{-1}$ for **1** in MeCN.[34] This quenching process is more than two orders of magnitude slower than in **6**

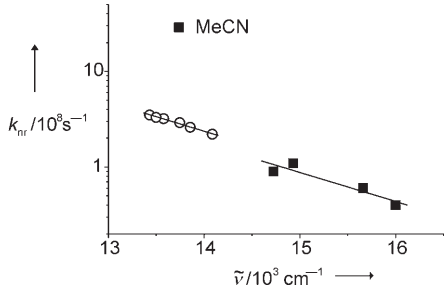

Figure 4. Plot of k_{nr} versus $\tilde{\nu}_{em}$ for **1** (■) and **4** (○). The fits contain all the data points for **4**, but excludes MeCN for **1**; the respective correlation coefficients are $r=0.996$ for **4** and 0.937 for **1**. The slopes of both fits are virtually identical with -3.05×10^{-4} for **4** and -3.04×10^{-4} for **1**.

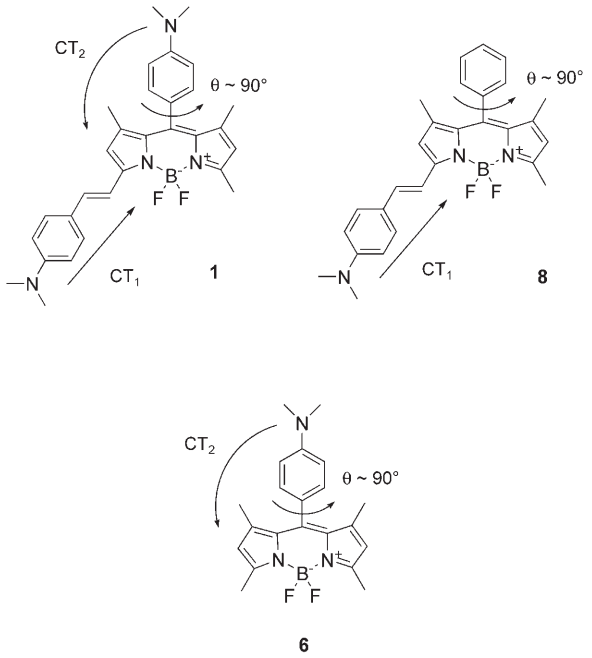

Scheme 4. Possible and competing charge transfer processes in **1**, **8**, and **6**. CT_1 in the planar conjugated chromophore is responsible for the bright emission; CT_2 between the virtually decoupled chromophore and the *meso* substituent is of a non-emitting nature. CT states such as those of CT_2 are usually characterized by a negligible oscillator strength ($f=0.0000$ in the present case, from the AM1 calculations), full charge separation, and an extremely high dipole moment (30 D in the present case) so that they are significantly stabilized in highly polar solvents and can be lower lying than the CT_1 state in solvents such as MeCN. For a detailed discussion of such competing processes in related compounds, see reference [53].

($330\ ns^{-1}$)[25] because the HOMO located on the BDP fragment becomes distinctly more positive (0.31 eV) when the chromophore system is extended by the (dimethylamino)-styryl group, whereas the energy of the MO located on the *meso* fragment increases to a smaller extent (Table 3).[20,21]

Table 3. Energy properties of the frontier molecular orbitals (MOs) of S_0 geometry-optimized **1**, **6**, and **7** (AM1, AMPAC V6.55).

	MO_{meso}[a] [eV]	HOMO[b] [eV]	LUMO[b] [eV]
1	−8.58 (HOMO-2)	−7.58	−1.54
7	−9.04 (HOMO-2)	−7.90	−1.54
6	−8.78 (HOMO-1)	−7.89	−1.48
Δ_{1-6}	0.20	0.31	−0.06
Δ_{7-6}	−0.26	−0.01	−0.06

[a] Molecular orbital located on the substituent in the *meso* position. [b] Both located on the BDP fragment.

The more-efficient quenching of **1** than of **2** in highly polar solvents is related to the electron-donor strength of the *meso* substituent. Whereas **2** shows oxidation potentials of E_P(ox, 8-hq) = 1020 mV (8-hq = 8-hydroxyquinoline) and E_P(ox, BDP) = 739 mV, the dimethylaniline group in **1** is oxidized much more readily ($E_{1/2}$(ox) = 492 mV; E_P(ox, BDP) = 748 mV).[35] Comparison of the oxidation waves with those of the 8-hq unit in **7** (E_P(ox) = 1027 mV) and the dimethylaniline group in **6** ($E_{1/2}$(ox) = 528 mV) further indicates that the introduction of a 3-(dimethylamino)styryl group has virtually no effect on the electron-donating strength of the *meso* substituent, supporting the MO considerations in the previous paragraph.[36–38]

Before presenting the pH-dependent spectroscopic properties of some of the dyes, it should be noted that especially the fused BDI dye **4** displays another advantageous aspect in terms of fluorescence applications. Whereas many NIR dyes with a longer polymethine chain in the chromophore (e.g. styryl dyes) suffer from rather high anisotropies ($\geq$ 0.05), **4** shows a considerably low fluorescence anisotropy (e.g. $r = 0.03$ in methanol). For comparison, $r = 0.07$ for **3** in the same solvent. Low anisotropies of the unperturbed dye in solution are favorable factors when such molecules are used as markers for biological superstructures in which the anisotropy is often strongly altered, that is, increased upon incorporation of the label in the restricted environment of a biomolecule.

pH-Dependent Absorption and Fluorescence Spectroscopy of Selected Dyes

Detailed protonation experiments were carried out in aqueous solution for **1**, **4**, **6**, and **8**. All four dyes are sufficiently soluble in water and carry one or two dimethylamino groups so that, in principle, they can be employed as pH indicators (acidic range) in the red/NIR spectral region. Table 4 collects the spectroscopic properties of the four dyes in the fully protonated and unprotonated state.

For all four dyes, the absorption band in water undergoes a red shift relative to that in methanol or acetonitrile (compare spectra of **1** in Figures 2 and 5). At the same time, the molar absorptivity of the $S_1 \leftarrow S_0$ absorption band is decreased to about 50% of that in MeCN, and the width of the band is roughly doubled, yielding comparable oscillator strengths. We have observed such hypsochromic and broadening effects before for a 1,3,5,7-tetramethyl-BDP derivative upon changing from organic solvents to water, and these effects can be attributed to the strong solvation tendency of water.[39] Besides the model compound **6**, which behaves very similarly to the BDP dye in reference [39], that is, shows dual fluorescence in water (Figure 5), the other three dyes are very weakly (**1**, Figure 5) or virtually nonfluorescent in neutral aqueous solution (**4** and **8**, Table 4). Apparently, the strong interaction of water molecules with the nitrogen atom of the 4-(dimethylamino)styryl group leads to a very efficient radiationless dissipation of the excitation energy. The dual fluorescence in the case of **6** can also be understood on the basis of strong hydrogen bonding, this time solely at the 8-dimethylanilino group. In water, the

Table 4. Spectroscopic and photophysical properties of neat and fully protonated **1**, **4**, **6**, and **8** in water at 298 K.

	λ_{abs} [nm]	λ_{em} [nm]	Φ_f	τ_f [ns]
1	578 (622)[a]	758	9×10^{-4}	<0.01
1-2H$^+$	557	565	0.55	3.56
4	722	n.d.[b]	n.d.[b]	n.d.[b]
4-H$^+$	664	675	0.27	2.51
6	499 (517)[a]	509/644[c]	0.02[c]	0.09/1.32[c]
6-H$^+$	498	511	0.58	3.68
8	578 (637)[a]	n.d.[b]	n.d.[b]	n.d.[b]
8-H$^+$	555	561	0.65	3.60

[a] Intense shoulder on the low-energy side. [b] Too weak to be reliably detectable. [c] Dual fluorescence with similar features as reported for the title dye in reference [39] with a Φ_f^{CT}/Φ_f^{LE} ratio of 11.6; see text for explanation.

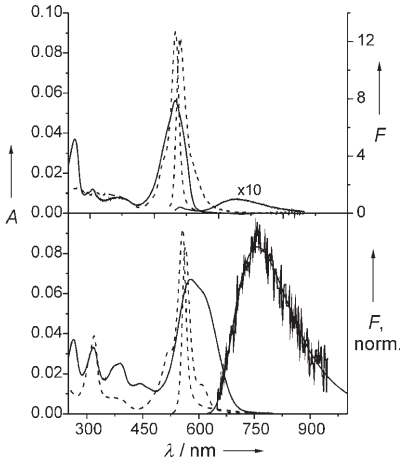

Figure 5. Absorption and fluorescence spectra of **6** (top) and **1** (bottom) in water at pH 6.4 (——) and pH 1.0 (-----) at 298 K. The emission spectrum of unprotonated **6** is magnified by a factor of 10; the fluorescence spectra of **1** and **1**-2H$^+$ (for the nature of this species, see text) were normalized for better comparison; for corresponding data, see Table 4.

electron-donating strength of that group decreases dramatically, so that the efficient charge-transfer process CT_2 (Scheme 4) is slowed down, and the fluorescence accordingly turned moderately on. The overall fluorescence Φ_f is 0.02 with 8% contribution from the BDP-localized or locally excited (LE) and 92% from the CT fluorescence. The fluorescence lifetime measurements performed for **6** in water support the CT features of dual fluorescence, as a precursor–successor relationship was found for LE and CT states (for a detailed description and formalism, see references [20,25,39]).

Subjecting the dyes to a pH titration leads to a different picture. In this case, the behavior of **4** and **8** is straightforward. Gradual acidification of the solution leads to the appearance of blue-shifted absorption spectra that show typical BDP features, such as narrow bands and a vibronic shoulder on the high-energy side. Accordingly, excitation of this species yields the characteristic, mirror-image resonant fluorescence band (Table 4; the spectral shapes are very similar to the dotted spectra in Figure 5). The fluorescence quantum yields and decay times, and hence k_r and k_{nr}, of the protonated species are very similar to those of the dyes in nonpolar solvents (Tables 4 versus 2). Protonation of the (dimethylamino)styryl group apparently switches off the CT_1 characteristics and transforms **4** and **8** into highly emitting dyes with entirely BDP-localized photophysical properties. The pK_S of **4** (1.97 ± 0.03) and **8** (1.16 ± 0.02) have been determined both photo- and fluorometrically, and the results of the two methods are in good agreement.[40]

Although the endpoint spectra (Figure 5) and data (Table 4) of **1** and **6** suggest a very similar behavior, remarkable observations were made especially for **1** during a pH titration. Compound **1** bears two potential protonation sites—the two dimethylamino groups, which differ slightly in basicity. Semiempirical calculations at the AM1 level and consideration of the resulting charge densities under assumptions detailed in reference [41] revealed that the charge on the dimethylamino group Q_{DMA} is larger for the 8-(dimethylamino)phenyl than for the 3-(dimethylamino)styryl moiety (0.012 versus 0.037). Consequently, protonation at the virtually decoupled group is expected to occur first and should be spectroscopically manifested in a reduction of the characteristic absorption band for the aniline group at 265 nm, with unaltered features in the other parts of the spectrum. Protonation at the other site should then entail the spectroscopic modulations described above for **4** and **8**.[42]

However, a pH titration of **1** in water showed an unusual course. The absorption decreases dramatically over the entire wavelength range (200–800 nm) between pH 5.5–2.5, and the blue solution discolored almost completely. At the same time, a blue precipitate is formed at the teflon stirrer bar, and flakes of the precipitate float on the surface of the titration solution. The addition of more acid to the solution gradually redissolves the precipitate, yet the solution becomes increasingly pink instead of blue. Figure 6 summarizes the observations in terms of a spectrophotometric titration curve at 540 nm. Clearly, two points of inflection are

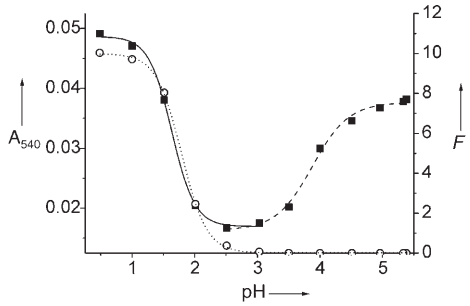

Figure 6. The pH titration curves of **1** in water. Black symbols represent absorption data and dashed and solid lines indicate the fits of both pK_S; white circles and dotted line represent data and fit of the fluorescence data.

distinguished and allow the determination of the corresponding pK_S values to be 3.88 ± 0.03 and 1.63 ± 0.02. The results are reproducible, and fluorescence titration curves support these unusual findings (Figure 6). A strong increase in emission is only noticed in the very acidic pH range, and the corresponding pK_S value amounts to 1.79 ± 0.01. All these features suggest that protonation occurs first at the *meso* (dimethylamino)phenyl group. The color of the compound/precipitate stays blue, and the fluorescence remains strongly quenched as one would expect only from protonation at the decoupled dimethylaniline group.[43] (Note that model **8** also shows no fluorescence at such pH values, Table 4.) Only in the second phase, below pH 2.5, does the pink color and strong fluorescence appear, which indicate the inhibition of the second CT_1 process from the (dimethylamino)styryl site (similar to **8**).

To verify the nature of the blue precipitate by a more direct method, we recorded IR spectra of neat **1**, the precipitate (monoprotonated **1**-H^+), and doubly protonated pink **1**-$2H^+$. In the case of **1**, only the absorptions for C–H stretching (peaks at 2803, 2857, 2917, and 2952 cm^{-1} for the aliphatic CH groups and three weaker bands at 3034, 3068, and 3093 cm^{-1} for alkenyl or aromatic CH groups) were observed between 2800–4000 cm^{-1}. For the blue precipitate, the spectra showed slight changes in the C–H stretching peaks and, most prominently, an additional band at 3295 cm^{-1}, indicative of the presence of the NH^+ group. In contrast, the doubly protonated pink species is very hygroscopic, and a broad band due to water was observed at $\approx$3500 cm^{-1}, strongly overlapping with a band at 3295 cm^{-1}, which indicates the presence of the NH^+ groups in **1**-$2H^+$. It thus seems that single protonation of **1** does not primarily affect the spectroscopic properties, but literally switches the lipophilicity of the dye. Despite the fact that an additional charge is introduced to an internally zwitterionic molecule, **1**-H^+ is distinctly more lipophilic than **1** or **1**-$2H^+$. The pH titrations of **6** in water support these findings, as the absorption spectrum also decreases over the entire wavelength range upon addition of acid. However, in this case, the fluorescence shows a concomitant increase in the BDP-localized band and a decrease in the CT band, and analysis of both types of data yields $pK_S = 3.11 \pm 0.01$.

Cation-Binding Features of 2 and 3

Since we are interested in the rational design of BDP/BDI-based probe molecules, in particular those derivatives with an analyte-responsive group in the *meso* position, which often show exceptional fluorescence switching features as an indication mode, we became intrigued by a report of Moon et al. on the signaling features of **7**.[23] In contrast to most of the probes that carry an electron-rich group in the *meso* position,[16,25,33,44] **7** is equipped with an 8-hq moiety, which is neither a strong electron donor nor acceptor (see above). Accordingly, **7** shows reasonable fluorescence in solvents ranging from hexane to acetonitrile. However, metal-ion binding at the 8-hq site is transduced by strong fluorescence quenching. Moon et al. attributed the quenching of the BDP fluorescence in the complex **7**–Hg^{2+} to the heavy atom effect of Hg^{2+} as well as to a photoinduced electron transfer (PET) from the 8-hq moiety in the phenolate state. Both assumptions, however, do not explain the distinct chromogenic response that these authors also found for **7**–Hg^{2+}.[23] We thus equipped **2** and **3** with the same receptor to investigate the mechanism of the complexation reaction of a positively charged species at a relatively electroneutral receptor group such as a 8-hydroxyquinoline moiety in the *meso* position.

The modulations of the spectroscopic properties of **2**, **3**, and model compound **7** were recorded as a function of the concentration of Hg^{2+} and/or Al^{3+} in acetonitrile and/or methanol. Since the fluorescence of neat **2** and **3** is already largely quenched in water, we relied on organic solvents for the present purposes. Al^{3+} was chosen as a representative metal ion that is readily complexed by the 8-hydroxyquinoline receptor but induces no heavy-atom effect.

Figure 7 combines selected effects of Hg^{2+}, Al^{3+}, and base on the absorption spectra of **2** and **7**. In all the cases, the cation induces a batho- and hypsochromic shift in absorption. Furthermore, whether Al^{3+} or Hg^{2+} is employed, none of the complexes formed show a measurable emission. The latter findings together with panels A and B in Figure 7 clearly show that the nature of the metal ion does not play a major role in fluorescence quenching. Both Hg^{2+} and Al^{3+} induce comparable spectral effects and lead to fluorescence quenching.[45] Moreover, a PET process from an anionic, phenolate-type 8-hq moiety to the BDP chromophore is also less likely to be responsible because abstraction of the proton of the 8-hq unit leads to slight hypsochromic shifts in absorption (Figure 7D), conceivable with an increase in electron density at the *meso* position of the BDP and BDI core.[20] Deprotonation of the 8-hq group converts this group from a weak to a stronger donor, entailing slightly blue-shifted absorption bands (607 for the anion versus 612 nm for the neutral dye, see Figure 7D). As the base-induced changes are distinctly different from the cation-induced changes, a PET can be ruled out as the cause of the lower fluorescence of the complexes. A similar yet more pronounced trend as shown for **2** in Figure 7D is found for **3** upon deprotonation in MeOH/H_2O (1:1 *v*/*v*): a hypsochromic shift from 716 to 705 nm.

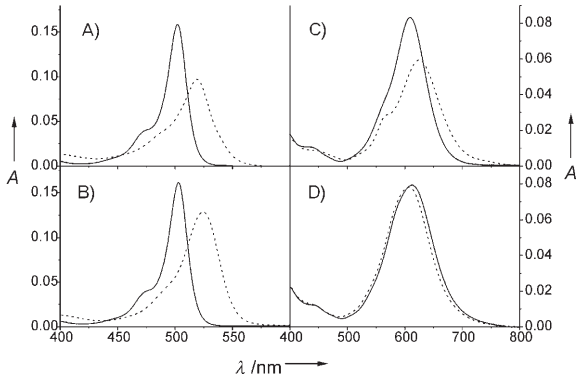

Figure 7. Absorption spectra: A) **7** (——) and **7**-Al^{3+} (-----) in MeCN; B) **7** (——) and **7**-Hg^{2+} (-----) in MeOH; C) **2** (——) and **2**-Hg^{2+} (-----) in MeCN; D) **2** (——) and **2** in the presence of triethylamine (4 mM) (-----) in MeOH/H_2O (1:1 *v*/*v*).

The electronic changes that occur upon complexation of the 8-hq moiety can be interpreted by employing quantum chemical calculations at the semiempirical level. As the metal ions employed in this case are often not sufficiently well parameterized in quantum chemical programs, we compared the neutral dyes **2**, **3**, and **7** with the corresponding structures in which the nitrogen atom of the 8-hq moiety is protonated. The results presented in the following section thus reflect only the expected trends.

For all three compounds, the lowest-energy oscillator-strong transition that is localized on the BDP core is a HOMO–LUMO transition in the unprotonated, yet a HOMO–LUMO+1 transition in the protonated dyes (Table 5). In the neat dyes, the LUMO+1 is then located on the 8-hq fragment. Thus, protonation (and most probably also complexation with a di- or even trivalent metal ion) of the nitrogen atom of the quinoline group leads to a reversal of the LUMO and LUMO+1 energy levels. Consequently, when an electron is excited from the HOMO to the LUMO+1 in the protonated or complexed dyes, it can be rapidly transferred to the empty orbital localized on the *meso* substituent. The quenching process therefore involves an ET from the BDP to the protonated/complexed 8-hq group. Accordingly, a light metal ion such as Al^{3+} and a

Table 5. Energy properties of the frontier molecular orbitals (MOs) of S_0 geometry-optimized **2**, **3**, and **7** and their corresponding analogues with an 8-hq group that is protonated at the quinolino nitrogen atom (AM1, AMPAC V6.55).

	HOMO[a] [eV]	LUMO [eV]	LUMO+1 [eV]	E_{S0-S1}[c] [cm^{-1}]
2	−7.61	−1.63[a]	−0.78[b]	19490
2-H^+	−9.50	−5.16[b]	−4.48[a]	16990
3	−7.40	−1.69[a]	−0.74[b]	18450
3-H^+	−9.17	−5.04[b]	−4.37[a]	15400
7	−7.90	−1.54[a]	−0.79[b]	20830
7-H^+	−10.67	−5.39[b]	−4.70[a]	20240

[a] Localized on BDP. [b] Localized on 8-hq. [c] Energy of the lowest oscillator-strong transition localized on the BDP core.

heavy metal ion such as Hg^{2+} induce similar modulations. The spectral shifts in absorption can again be understood on the basis of the electron-density redistribution that occurs upon excitation (see above). The protonated or complexed 8-hq group represents a strong electron acceptor, and the dyes thus display pronounced bathochromic shifts in absorption (Table 5). As this modulation of the electronic properties of the compounds is independent of the auxochrome and occurs similarly in **2**, **3**, and **7**, these findings are an essential rule that has to be considered in the design of *meso*-substituted BDP probes.

Conclusions

In conclusion, we have presented various novel BDP and BDI dyes that absorb in the red visible and emit in the NIR spectral range. Solvatochromic and solvatokinetic data have identified all the four fluorophores as principally very potent emitters in this advantageous wavelength range. By using only styryl extensions on the pyrromethene core, the syntheses are straightforward. In the case of a BDI core the fluorophore exhibits a favorably low fluorescence anisotropy while still displaying fluorescence lifetimes of several nanoseconds. Moreover, the attachment of different addressable substituents to the *meso* position provided insight into the signaling processes of such long-wave fluorophores and classic BDP dyes. Dye **1** showed the most remarkable behavior as its lipophilicity could be switched by protonation. Furthermore, **4** presents a red-visible/NIR pH indicator with bright fluorescence. In contrast, **2** and **3** helped to identify the mechanisms at play when a considerably electroneutral receptor is attached to the core at the *meso* position, and binding of metal ions leads to rather pronounced shifts in absorption and strong quenching of the fluorescence. Preliminary studies also suggest that for, for example, *meso*-phenyl derivative of **3** might be an equally potent pH indicator as **4**. The unique features of the BDP and BDI chromophores further guarantee that despite the role that internal conversion naturally plays in this wavelength range, strongly emitting dyes can be developed. At least in the case of styryl groups, the presence of flexible single and double bonds does not induce quenching processes such as excited-state *trans–cis* photoisomerization or twisted intramolecular charge-transfer (TICT) reactions that can lead to additional nonradiative losses, as is the case with many UV/Vis chromophores.[46] We thus anticipate that NIR BDP and BDI dyes will be powerful competitors of cyanine dyes in the future.

Experimental Section

General

All syntheses were carried out under an inert atmosphere. Unless otherwise noted, all chemicals and solvents were of commercial reagent grade and used without further purification. Dry dichloromethane was freshly distilled over CaH_2 under nitrogen. Triethylamine was obtained by simple distillation. Dry toluene was distilled from sodium/benzophenone under an inert atmosphere. Column chromatography and TLC were performed on C-200 (Wakogel) and Kieselgel 60F254 (Merck), respectively. Elemental analyses for C, H, and N were performed on a Perkin–Elmer 240 C elemental analyzer. The IR spectra were recorded on a VECTOR 22 spectrophotometer with KBr discs in the 4000–400 cm^{-1} region. ^1H NMR spectra were recorded in $CDCl_3$ on a Bruker ARX500 spectrometer at ambient temperature. NMR chemical shifts are expressed relative to TMS as the internal standard. MALDI-TOF MS and HRMS (FAB) measurements were carried out at Ehime University, Matsuyama, Japan.

All the solvents employed for the spectroscopic measurements were of UV spectroscopic grade (Aldrich). Metal perchlorates purchased from Merck, Acros, and Aldrich were of the highest purity available and were dried as described previously.[29] DCM was purchased from Lambda Physik GmbH, Göttingen, Germany.

Syntheses

1: Indacene **6** (73 mg, 0.2 mmol)[18] and 4-dimethylaminobenzaldehyde (45 mg, 0.3 mmol) were heated at reflux for 48 h in a mixed solution of toluene (5 mL), glacial acetic acid (0.15 mL), and piperidine (0.18 mL) in the presence of a small amount of activated 4-Å molecular sieves.[21] The mixture was cooled to room temperature, the solvents were removed under vacuum, and the crude product was purified by column chromatography on silica gel by elution with ethyl acetate/petroleum ether (20%). The blue fraction was collected and recrystallized from chloroform/methanol to give **1** as brown shining needles (15%). M.p. > 250 °C; IR (KBr): $\tilde{\nu}$ = 1593, 1530 (C=C, C=N), 1164 cm^{-1} (B-F); ^1H NMR (500 MHz, $CDCl_3$, 25 °C, TMS): δ = 7.54–7.50 (m, 3H), 7.23–7.20 (m, 1H), 7.13–7.11 (m, 2H), 6.82–6.70 (m, 4H), 6.61 (s, 1H), 5.99 (s, 1H), 3.05 (s, 12H), 2.61 (s, 3H), 1.55 (s, 3H), 1.51 ppm (s, 3H); ^{13}C NMR (100 MHz, $CDCl_3$) δ = 153.8, 150.5, 150.2, 138.5, 137.8, 137.2, 136.5, 133.2, 132.9, 132.0, 129.4, 128.8, 128.6, 127.8, 125.7, 122.9, 114.4, 112.3, 40.1, 30.9, 29.8, 14.2 ppm; MS (MALDI-TOF): calcd for $C_{30}H_{33}BF_2N_4$: 498.28; found: 498.91; elemental analysis: calcd (%) for $C_{30}H_{33}BF_2N_4$: C 72.29, H 6.67, N 11.24; found: C 72.46, H 6.59, N 11.42.

2: 4-Dimethylaminobenzaldehyde (39 mg, 0.26 mmol) and **7** (78 mg, 0.2 mmol) were heated at reflux for 15 h in a mixed solution of dry toluene (20 mL), glacial acetic acid (0.7 mL), and piperidine (0.8 mL) in the presence of a small amount of activated 4-Å molecular sieves.[21] The reaction was monitored by TLC (eluent ethyl acetate/petroleum ether (20%)). The mixture was cooled to room temperature, the solvents were removed under vacuum, and the crude product was placed on a silica column and eluted with ethyl acetate/petroleum ether (20%). The blue fraction was collected and recrystallized from chloroform/methanol to give **2** as a blue powder (17%). M.p. > 250 °C; ^1H NMR (500 MHz, $CDCl_3$, 25 °C, TMS): δ = 8.33 (d, J = 8.4 Hz, 1H), 8.11 (s, 1H), 7.60–7.54 (m, 6H), 7.46 (d, J = 8.4 Hz, 1H), 7.27 (d, J = 7.3, 1H), 6.75 (s, 2H), 6.64 (s, 1H), 6.01 (s, 1H), 3.06 (s, 6H), 2.64 (s, 3H), 1.28 (s, 3H), 1.24 ppm (s, 3H); ^{13}C NMR (100 MHz, $CDCl_3$): δ = 155.8, 152.5, 152.2, 142.2, 140.0, 138.5, 137.8, 137.2, 135.5, 133.2, 130.9, 129.4, 128.8, 127.8, 122.9, 120.6, 118.0, 117.9, 114.4, 112.9, 112.3, 110.9, 40.3, 30.9, 29.7, 14.3 ppm; MS (MALDI-TOF): calcd for $C_{31}H_{29}BF_2N_4O$: 522.4; found: 522.20; elemental analysis: calcd (%) for $C_{31}H_{29}BF_2N_4O$: C 71.27, H 5.60, N 10.72; found: C 71.46, H 5.49, N 10.52.

3: 4-Dimethylaminobenzaldehyde (39 mg, 0.26 mmol) and **7** (78 mg, 0.2 mmol) were heated at reflux for 7 days in a mixed solution of dry toluene (20 mL), glacial acetic acid (0.7 mL), and piperidine (0.8 mL) in the presence of a small amount of activated 4-Å molecular sieves.[21] The reaction was monitored by TLC (eluent ethyl acetate/petroleum ether (50%)). The mixture was cooled to room temperature, the solvents were removed under vacuum, and the crude product was purified by column chromatography on silica gel eluted with ethyl acetate/petroleum ether (50%). The green fraction was collected and recrystallized from chloroform/methanol to give **3** as a metallic, shiny solid (25%). M.p. > 250 °C; ^1H NMR (500 MHz, $CDCl_3$, 25 °C, TMS): δ = 8.32 (d, J = 8.4 Hz, 1H), 8.15 (s, 1H), 7.62–7.57 (m, 8H), 7.46 (d, J = 8.4 Hz, 1H), 7.30–7.22 (m,

3H), 6.77–6.64 (m, 6H), 3.07 (s, 12H), 1.28 ppm (s, 6H); ^{13}C NMR (100 MHz, $CDCl_3$): δ = 155.8, 152.5, 142.2, 140.0, 138.5, 137.2, 135.5, 133.2, 130.9, 129.4, 128.8, 127.8, 122.9, 120.6, 118.0, 117.9, 114.4, 112.9, 112.3, 110.9, 40.4, 30.9 ppm; MS (MALDI-TOF): calcd for $C_{40}H_{38}BF_2N_5O$: 653.31; found: 653.48; elemental analysis: calcd (%) for $C_{40}H_{38}BF_2N_5O$: C 73.51, H 5.86, N 10.72; found: C 73.46, H 5.69, N 10.62.

4: Compound **10** (66 mg, 0.1 mmol)[20] and 4-dimethylaminobenzaldehyde (20 mg, 0.13 mmol) were heated at reflux for 26 h in a mixed solution of dry toluene (5 mL), glacial acetic acid (0.1 mL), and piperidine (0.1 mL) in the presence of a small amount of activated 4-Å molecular sieves.[21] The solution was cooled to room temperature, and the mixture was purified by column chromatography on silica gel eluted with dichloromethane/methanol (10%). The blue fraction was collected and recrystallized from chloroform/methanol to give **4** as a blue powder (17%). M.p. > 250°C; ^{1}H NMR (400 MHz, $CDCl_3$, 25°C, TMS): δ = 8.14–8.12 (d, J = 8.3 Hz, 1H), 7.98–7.87 (m, 1H), 7.70–7.60 (m, 4H), 7.22–7.21 (m, 2H), 7.13–6.99 (m, 5H), 6.79–6.74 (m, 2H), 6.41–6.39 (m, 1H), 6.36–6.33 (m, 1H), 4.31 (m, 2H), 4.09–4.04 (m, 4H), 3.87–3.80 (m, 10H), 3.06 (s, 6H), 2.95 ppm (s, 3H); ^{13}C NMR (100 MHz, $CDCl_3$): δ = 151.0, 150.9, 150.3, 149.6, 149.5, 137.7, 137.2, 129.0, 129.0, 128.9, 128.6, 128.2, 127.9, 125.6, 124.9, 124.8, 123.8, 123.5, 123.5, 122.3, 121.9, 121.8, 121.7, 121.6, 121.5, 113.7, 113.5, 112.2, 112.1, 71.1, 70.9, 70.2, 70.1, 69.4, 69.1, 68.6, 68.4, 40.4, 29.8 ppm; HRMS (FAB): calcd for $C_{42}H_{42}BF_2N_3O_5$: 717.3184; found: 717.3191; elemental analysis: calcd (%) for $C_{42}H_{42}BF_2N_3O_5 \cdot H_2O$: C 68.57, H 6.03, N 5.71; found: C 68.74, H 6.16, N 5.60.

5, **6**, **8**–**10**, and BTC were synthesized as reported previously,[20,21,25,29] and **7** was prepared by a route adopted from reference [23].

Crystal-Structure Determination

A single crystal of compound **1** was selected under a microscope and mounted on a glass fiber. The unit-cell parameters and data were collected on a Bruker Smart Apex CCD diffractometer with graphite monochromated $Mo_{K\alpha}$ radiation (λ = 0.71073 Å) in the ω–2θ scan mode. The data were corrected for Lorenz and polarization effects. The structure was solved by direct methods and refined on F^2 by full-matrix least-squares methods with the SHELXTL-2000 program package.[47] CCDC-281155 contains the supplementary crystallographic data for this paper. These data can be obtained free of charge from The Cambridge Crystallographic Data Centre via www.ccdc.cam.ac.uk/conts/retrieving.html (or from the Cambridge Crystallographic Data Centre, 12, Union Road, Cambridge CB21EZ, UK; fax: (+44) 1223-336-033; or deposit@ccdc.cam.ac.uk).

Steady-State Absorption and Fluorescence Spectroscopy

Steady-state absorption, fluorescence measurements, and fluorescence titrations were carried out on a Cary 5000 UV/Vis–NIR spectrophotometer, a Spectronics Instrument 8100 spectrofluorometer, and a Perkin–Elmer LS50B spectrofluorometer, respectively. For all measurements, the temperature was kept constant at 298 ± 2 K. Unless otherwise noted, only dilute solutions with an absorbance of less then 0.1 at the absorption maximum were used. Fluorescence experiments were performed with a 90° standard geometry, with polarizers set at 54.7° for emission and 0° for excitation. The fluorescence quantum yields (Φ_f) of **6** and **7** have either been reported previously[23,25] or were determined relative to fluorescein 27 in NaOH (0.1 N) (Φ_f = 0.90 ± 0.03).[48] For **5**, data additional to those reported in reference [21] were determined relative to Rhodamine 101 in ethanol (Φ_f = 1.00 ± 0.02).[49] The latter dye was also used to construct a chain of transfer standards to the NIR region, to account for inconsistencies in fluorescence quantum-yield data reported in the literature so far. For this purpose, cresyl violet in methanol, oxazine 1 in ethanol, and cryptocyanine in ethanol were used as the chemical transfer standards. By employing the traceably characterized Spectronics Instrument 8100 spectrofluorometer,[50] the fluorescence quantum yield of cryptocyanine, for instance, was determined to 0.013 ± 0.001 instead of 0.007 as published previously.[51] These red/NIR dyes were then used in the appropriate wavelength range as relative standards for **1**–**4**. All the fluorescence spectra presented herein were spectrally corrected.[50] The uncertainties of the measurements were determined to be ±5% (for $\Phi_f > 0.2$), ±10% (for $0.2 > \Phi_f > 0.02$), and ±20% (for $0.02 > \Phi_f$).

Time-Resolved Fluorescence Spectroscopy

Fluorescence lifetimes (τ_f) were determined by a unique customized laser impulse fluorometer with picosecond time resolution which we described in earlier publications.[20,52] The fluorescence was collected at right angles (polarizer set at 54.7°; monochromator with spectral bandwidths of 4, 8, and 16 nm), and the fluorescence decays were recorded with a modular single-photon timing unit.[20] At typical instrumental response functions of fwhm ≈ 25–30 ps, the time division was 4.8 ps channel^{-1}, and the experimental accuracy amounted to ±3 ps. The laser beam was attenuated by using a double prism attenuator from LTB, and typical excitation energies were in the nanowatt to microwatt range (average laser power). The fluorescence lifetime profiles were analyzed by using the software package Global Unlimited V2.2 (Laboratory for Fluorescence Dynamics, University of Illinois). The goodness of the fit of the single decays as judged by reduced chi-squared (χ_R^2) and the autocorrelation function $C(j)$ of the residuals was always below $\chi_R^2 < 1.2$. For all the dyes, decays were recorded at three different emission wavelengths over the BDP-type emission spectrum and analyzed globally. Such a global analysis of decays recorded at different emission wavelengths implies that the decay times of the species are linked, while the program varies the preexponential factors and lifetimes until the changes in the error surface (χ^2 surface) are minimal, that is, convergence is reached. The fitting results are judged for every single decay (local χ_R^2) and for all the decays (global χ_R^2). The errors for all the global analytical results presented herein were below a global $\chi_R^2 = 1.2$.

Measurements of pH Values

For every step of the pH titration, small amounts of $HClO_4$ (11.2 M, 70% by weight) were added (microliter pipette, Eppendorf) to a solution (50 mL) containing the dye (≈2 μM). The latter was added in small amounts (typically 1–2 vol% of the stock solution in acetonitrile). The mixture was stirred for 3 min, and an aliquot of the solution (3 mL) was transferred to a 10-mm quartz cuvette and stirred for a further 1 min. The pH value was monitored with a digital pH meter (WTW pH 537) equipped with a glass electrode (Mettler Toledo InLab 423). Calibration of the instrument was performed with standard aqueous solutions of pH 1.68, 4.01, 6.86, and 9.18 from WTW.

IR Spectroscopy

With respect to the elucidation of the nature of the blue precipitate formed under mildly acidic conditions during a pH titration of **1** in water, a KBr pellet with **1** was prepared and measured on a Bruker IF66v FT-IR spectrometer with vacuum in transmission mode. For the preparation of the sample **1**-H$^+$, an aqueous solution of **1** was acidified with $HClO_4$ until a blue precipitate appeared and the solution turned colorless. The blue precipitate formed on the magnetic stirrer bar was prepared further for measurements by simply allowing the stirrer to dry in a normal atmosphere. The precipitate was removed from the stirrer bar with a spatula and then directly measured under a microscope coupled to a Bruker Equinox 55 (IR-Scope II) FTIR spectrometer in transmission mode, with a KBr window. Blank teflon was also measured to account for possible artifacts. **1**-2H$^+$ was prepared by dissolving **1** in CH_2Cl_2 in an extraction funnel and subsequently adding an aqueous solution of $HClO_4$. After the two phases were mixed, the color changed from blue to pink in solution in dichloromethane. The organic phase was separated, and dichloromethane was evaporated. The IR spectra of the pink solid were then obtained with the microscope used for **1**-H$^+$.

Electrochemistry

Selected redox properties were studied by cyclic voltammetry in TBAP (tetra-*n*-butylammonium perchlorate) (0.1 M) in acetonitrile on a Perkin–Elmer electrochemical analysis system model 283 with a platinum disk as the working electrode, Ag/AgCl as the quasi-reference electrode, and a platinum wire as the counterelectrode. Redox potentials were referenced internally against ferrocenium/ferrocene (Fc$^+$/Fc). All measurements

were performed under an inert atmosphere with a scan rate of 250 $mV\,s^{-1}$ at room temperature.

Acknowledgements

Financial support by the National Natural Science Foundation of China (No. 20401009 and 20531040), the Natural Science Foundation of Jiangsu Province (No. BK2004414), the Ministry of Chinese Education (research grant No. 0205133119), the Fok Ying Tung Education Foundation (No. 104013), the Alexander von Humboldt Foundation, and the BAM PhD program is highly appreciated. We are indebted to Dr. J. Kneipp and A. Kohl from BAM Div. I.3 for the IR measurements as well as to Dr. T. Okujima and Prof. N. Ono from Ehime University, Matsuyama, for MALDI-TOF MS measurements.

[1] J. Fabian, H. Nakazumi, M. Matsuoka, *Chem. Rev.* **1992**, *92*, 1197–1226.
[2] S. Dähne, *J. Imaging Sci. Technol.* **1994**, *38*, 101–117.
[3] M. Matsuoka, *Mol. Cryst. Liq. Cryst. Sci. Technol. Sect. A* **1993**, *224*, 85–94.
[4] J. Fabian, *J. Prakt. Chem.* **1991**, *333*, 197–222.
[5] S. McWhorter, S. A. Soper, *Electrophoresis* **2000**, *21*, 1267–1280.
[6] A. R. Swamy, M. I. Danesvar, L. Evans, L. Strekowski, N. Narayanan, F. Szurdoki, I. Wengatz, B. D. Hammock, G. Patonay, *ACS Symp. Ser.* **1997**, *657*, 146–161.
[7] M. Gurfinkel, S. Ke, X. X. Wen, C. Li, E. M. Sevick-Muraca, *Dis. Markers* **2003**, *19*, 107–121.
[8] E. Dekker, P. Fockens, *Eur. J. Gastroenterol. Hepatol.* **2005**, *17*, 803–808.
[9] B. Ballou, L. A. Ernst, A. S. Waggoner, *Curr. Med. Chem.* **2005**, *12*, 795–805.
[10] K. Licha, C. Olbrich, *Adv. Drug Delivery Rev.* **2005**, *57*, 1087–1108.
[11] Y. B. Wang, J. H. Yang, X. Wu, L. Li, S. Sun, B. Y. Su, Z. S. Zhao, *Anal. Lett.* **2003**, *36*, 2063–2094.
[12] N. Tyutyulkov, J. Fabian, A. Mehlhorn, F. Dietz, A. Tadjer, *Polymethine Dyes*, St. Kliment Ohridski University Press, Sofia, **1991**.
[13] D. F. O'Brien, T. M. Kelly, L. F. Costa, *Photogr. Sci. Eng.* **1974**, *18*, 76–84.
[14] R. E. Pagano, O. C. Martin, H. C. Kang, R. P. Haugland, *J. Cell Biol.* **1991**, *113*, 1267–1279; J. Karolin, L. B.-Å. Johansson, L. Strandberg, T. Ny, *J. Am. Chem. Soc.* **1994**, *116*, 7801–7806; T. G. Pavlopoulos, *Prog. Quantum Electron.* **2002**, *26*, 193–224. BDP labels are commercially available under their trademark name, bodipy, from Molecular Probes, http://probes.invitrogen.com/.
[15] T. Gareis, C. Huber, O. S. Wolfbeis, J. Daub, *Chem. Commun.* **1997**, 1717–1718; F. Bergström, I. Mikhalyov, P. Hägglöf, R. Wortmann, T. Ny, L. B.-Å. Johansson, *J. Am. Chem. Soc.* **2002**, *124*, 196–204; C. Goze, G. Ulrich, L. Charbonnière, M. Cesario, T. Prangé, R. Ziessel, *Chem. Eur. J.* **2003**, *9*, 3748–3755; Y. Gabe, Y. Urano, K. Kikuchi, H. Kojima, T. Nagano, *J. Am. Chem. Soc.* **2004**, *126*, 3357–3367; G. C. Ping, B. M. Zhu, M. Jabasini, F. Xu, H. Oka, H. Sugihara, Y. Baba, *Anal. Chem.* **2005**, *77*, 7282–7287.
[16] K. Rurack, M. Kollmannsberger, U. Resch-Genger, J. Daub, *J. Am. Chem. Soc.* **2000**, *122*, 968–969.
[17] F. Li, S. I. Yang, Y. Ciringh, J. Seth, I. C. H. Martin, D. L. Singh, D. Kim, R. R. Birge, D. F. Bocian, D. Holten, J. S. Lindsey, *J. Am. Chem. Soc.* **1998**, *120*, 10001–10017; H. Imahori, H. Norieda, H. Yamada, Y. Nishimura, I. Yamazaki, Y. Sakata, S. Fukuzumi, *J. Am. Chem. Soc.* **2001**, *123*, 100–110; R. Y. Lai, A. J. Bard, *J. Phys. Chem. B* **2003**, *107*, 5036–5042; F. D'Souza, P. M. Smith, M. E. Zandler, A. L. McCarty, M. Itou, Y. Araki, O. Ito, *J. Am. Chem. Soc.* **2004**, *126*, 7898–7907; C. Trieflinger, H. Röhr, K. Rurack, J. Daub, *Angew. Chem.* **2005**, *117*, 7104–7107; *Angew. Chem. Int. Ed.* **2005**, *44*, 6943–6947; H. Röhr, C. Trieflinger, K. Rurack, J. Daub, *Chem. Eur. J.* **2006**, *12*, 689–700.
[18] M. Kollmannsberger, T. Gareis, S. Heinl, J. Breu, J. Daub, *Angew. Chem.* **1997**, *109*, 1391–1393; *Angew. Chem. Int. Ed. Engl.* **1997**, *36*, 1333–1335;.
[19] H. Kim, A. Burghart, M. B. Welch, J. Reibenspies, K. Burgess, *Chem. Commun.* **1999**, 1889–1890; J. Chen, J. Reibenspies, A. Derecskei-Kovacs, K. Burgess, *Chem. Commun.* **1999**, 2501–2502; K. Yamada, T. Toyota, K. Takakura, M. Ishimaru, T. Sugawara, *New J. Chem.* **2001**, *25*, 667–669; A. Gossauer, F. Nydegger, T. Kiss, R. Sleziak, H. Stoeckli-Evans, *J. Am. Chem. Soc.* **2004**, *126*, 1772–1780; W. Zhao, E. M. Carreira, *Angew. Chem.* **2005**, *117*, 1705–1707; *Angew. Chem. Int. Ed.* **2005**, *44*, 1677–1679.
[20] Z. Shen, H. Röhr, K. Rurack, H. Uno, M. Spieles, B. Schulz, G. Reck, N. Ono, *Chem. Eur. J.* **2004**, *10*, 4853–4871.
[21] K. Rurack, M. Kollmannsberger, J. Daub, *Angew. Chem.* **2001**, *113*, 396–399; *Angew. Chem. Int. Ed.* **2001**, *40*, 385–387.
[22] K. Rurack, M. Kollmannsberger, J. Daub, *New J. Chem.* **2001**, *25*, 289–292.
[23] S. Y. Moon, N. R. Cha, Y. H. Kim, S.-K. Chang, *J. Org. Chem.* **2004**, *69*, 181–183.
[24] C. L. Picou, E. D. Stevens, M. Shah, J. H. Boyer, *Acta Crystallogr. Sect. C* **1990**, *46*, 1148–1150; N. Kuhn, A. Kuhn, M. Speis, D. Blaser, R. Boese, *Chem. Ber.* **1990**, *123*, 1301–1303.
[25] M. Kollmannsberger, K. Rurack, U. Resch-Genger, J. Daub, *J. Phys. Chem. A* **1998**, *102*, 10211–10220.
[26] Y. Fujimoto, N. Katayama, Y. Ozaki, S. Yasui, K. Iriyama, *J. Mol. Struct.* **1992**, *274*, 183–195.
[27] The data are plotted according to $\Delta\tilde{\nu}_{abs-em} = \Delta\tilde{\nu}^{vac}_{abs-em} + \frac{2(\mu_e-\mu_g)^2}{hc_0a_O^3}\left(f(\varepsilon_r) - f(n^2)\right)$ with $f(\varepsilon) = \frac{\varepsilon-1}{2\varepsilon+1}$, $f(n^2) = \frac{n^2-1}{2n^2+1}$ (μ_e and μ_g are the dipole moments in the excited and ground states, respectively, ε = dielectric constant, n = refractive index, h = Planck constant, c_0 = speed of light in a vacuum, a_O = Onsager cavity radius: E. Lippert, *Z. Naturforsch.* **1955**, *10a*, 541–545; E. Lippert, *Z. Elektrochem.* **1957**, *61*, 962–975; N. Mataga, Y. Kaifu, M. Koizumi, *Bull. Chem. Soc. Jpn.* **1956**, *29*, 465–470). The value of a_O was estimated from the AM1-optimized ground-state geometry and further assumptions proposed by Lippert.
[28] The dipole moments of **1**–**4** in the ground state were determined as 4.5, 4.3, 2.7, and 3.6 D for the optimized ground-state geometry by semiempirical AM1 calculations.
[29] K. Rurack, J. L. Bricks, G. Reck, R. Radeglia, U. Resch-Genger, *J. Phys. Chem. A* **2000**, *104*, 3087–3109.
[30] M. Meyer, J. C. Mialocq, *Opt. Commun.* **1987**, *64*, 264–268.
[31] J. B. Birks, *Photophysics of Aromatic Molecules*, Wiley-Interscience, London, **1970**. This effect can be accounted for by taking the reduced rate constant $\kappa_f = \frac{k_f}{\langle n^3\tilde{\nu}^3_{em}\rangle}$ with $\langle n^3\tilde{\nu}^3_{em}\rangle \approx n^3\frac{\sum\tilde{\nu}^3_{em}I_{\tilde{\nu}_{em}}}{\sum I_{\tilde{\nu}_{em}}}$ and $k_f = \frac{\Phi_f}{\tau_f}$ as a measure (n = refractive index of the solvent, $\tilde{\nu}_{em}$ = emission wavenumber, $I_{\tilde{\nu}_{em}}$ = emission intensity).
[32] W. Siebrand, *J. Chem. Phys.* **1967**, *46*, 440–447.
[33] M. Kollmannsberger, K. Rurack, U. Resch-Genger, W. Rettig, J. Daub, *Chem. Phys. Lett.* **2000**, *329*, 363–369.
[34] This assumption is considered to be valid, because excited-state processes such as photoisomerization or intersystem crossing do not play a prominent role in BDP and BDI photophysics.[20]
[35] Redox waves denoted E_p are irreversible, $E_{1/2}$ are reversible. The corresponding reduction potentials of the BDP units are $E_p(red) = -1747$ mV for **1** and $E_p(red) = -1620$ mV for **2**.
[36] These data also suggest that the 8-hq unit should quench the fluorescence less, and the decrease in Φ_f of **2** upon changing from CH_2Cl_2 to MeCN/MeOH is thus not yet understood.
[37] The twofold decrease in Φ_f of **2** upon changing from Bu_2O to hexane (Table 2) is also not yet understood. Such phenomena have been reported frequently for various BDP derivatives in various alkane solvents, for example: F. López Arbeloa, T. López Arbeloa, I. López Arbeloa, *J. Photochem. Photobiol. A* **1999**, *121*, 177–182; J. Banuelos Prieto, F. López Arbeloa, V. Martinez Martinez, T. Arbeloa Lopez, F. Amat-Guerri, M. Liras, I. López Arbeloa, *Chem. Phys. Lett.* **2004**, *385*, 29–35; M. Baruah, W. Qin, N. Basaric, W. M. De

Borggraeve, N. Boens, *J. Org. Chem.* **2005**, *70*, 4152–4157; W. Qin, T. Rohand, M. Baruah, A. Stefan, M. Van der Auweraer, W. Dehaen, N. Boens, *Chem. Phys. Lett.* **2006**, *420*, 562–568; the mechanistic interpretations are not consistent, that is, they range from specific solute–solvent effects through molecular rigidity to intersystem crossing.

[38] The benzocrown unit that was used in **4** to promote the water solubility of the BDI dye is also only a considerably weak electron donor ($E_{1/2}(\mathrm{ox}) = 1150$ mV)[33] and hence does not quench the intense emission of **4** in MeCN or MeOH. Accordingly, the spectroscopic features of **4** are also not affected by the presence of alkali and alkaline-earth metal ions, tested here for millimolar concentrations of K^+ and Ca^{2+}; see also references [20,33].

[39] J. L. Bricks, A. Kovalchuk, C. Trieflinger, M. Nofz, M. Büschel, A. I. Tolmachev, J. Daub, K. Rurack, *J. Am. Chem. Soc.* **2005**, *127*, 13522–13529.

[40] To assess the generality of the effect of protonation, spectrophotometric and steady-state fluorometric pH titrations were also performed for **3**. The neat dye displays a broad band with an absorption maximum at 743 nm in water, and the species in which both potential ICT donor sites are protonated (pH ≈ 0) absorbs with a characteristically narrow, cyanine-like band at 645 nm. However, most probably due to the influence of the 8-hydroxyquinoline moiety under strongly acidic conditions, the typical mirror-image-shaped emission with a maximum at 657 nm is only rather weak. (The peculiarities of 8-hydroxyquinoline as a substituent in the *meso* position are discussed in a separate section below.) Nonetheless, we anticipate that an analogue of **3** with a phenyl group or, for instance, a benzocrown in the *meso* position should show similar proton-induced "light-up" features as **4** does.

[41] K. Rurack, M. Sczepan, M. Spieles, U. Resch-Genger, W. Rettig, *Chem. Phys. Lett.* **2000**, *320*, 87–94.

[42] Notably, only gradual changes were observed when **1** was titrated with $HClO_4$ in neat acetonitrile or in acetonitrile/water (1:1 *v*/*v*), and it was not possible to discriminate between the two protonation sites upon different changes in different regions of the absorption spectrum (Figure S1 in the Supporting Information). Additionally, the appearance of the typical BDP emission at approximately 560 nm, which indicates the inhibition of the CT_1 process, occurred concomitantly. The two pK_S values of both dimethylamino groups are apparently too similar in organic and mixed aqueous solutions to be unequivocally distinguished from one another, and the first protonation of **1** in such solvents or mixtures occurs statistically at both sites.

[43] Owing to the precipitation of this species, quantitative analyses of the changes in the aniline absorption band in the $5.5 > pH > 2.5$ range did not yield very reliable results for the more basic p*K* values.

[44] T. Nishioka, T. Arimura, Y. Suga, S. Murata, M. Tachiya, M. Goto, *Bull. Chem. Soc. Jpn.* **2001**, *74*, 2435–2436; Y. K. Wu, X. J. Peng, B. C. Guo, J. L. Fan, Z. C. Zhang, J. Y. Wang, A. J. Cui, Y. L. Gao, *Org. Biomol. Chem.* **2005**, *3*, 1387–1392; N. Basaric, M. Baruah, W. Qin, B. Metten, M. Smet, W. Dehaen, N. Boens, *Org. Biomol. Chem.* **2005**, *3*, 2755–2761.

[45] When **2**-Al^{3+} or **3**-Al^{3+} are excited at 370 nm, at the absorption maximum of the 8-hq-Al^{3+} complex, the typical emission of the complex between 400 and 600 nm ($\lambda_{max} \approx 495$ nm) is strongly quenched owing to efficient energy transfer to the BDP. As **2** and **3** are also only weakly fluorescent in highly polar (protic) solvents, the yield of BDP emission upon excitation at 370 nm is also considerably low, and such molecules do not qualify as FRET (fluorescence resonant energy transfer) probes.

[46] W. Rettig, *Top. Curr. Chem.* **1994**, *169*, 253–299.

[47] Bruker (2000). Smart, Saint, Sadabs and Shelxtl. Bruker AXS Inc., Madison, Wisconsin, USA, **2000**.

[48] J. Olmsted III, *J. Phys. Chem.* **1979**, *83*, 2581–2584.

[49] D. F. Eaton, *Pure Appl. Chem.* **1988**, *60*, 1107–1114.

[50] J. Hollandt, R. D. Taubert, J. Seidel, U. Resch-Genger, A. Gugg-Helminger, D. Pfeifer, C. Monte, W. Pilz, *J. Fluoresc.* **2005**, *15*, 301–313; U. Resch-Genger, D. Pfeifer, C. Monte, W. Pilz, A. Hoffmann, M. Spieles, K. Rurack, J. Hollandt, D. Taubert, B. Schönenberger, P. Nording, *J. Fluoresc.* **2005**, *15*, 315–336.

[51] D. N. Dempster, T. Morrow, R. Rankin, G. F. Thompson, *Chem. Phys. Lett.* **1973**, *18*, 488–492.

[52] U. Resch, K. Rurack, *Proc. SPIE-Int. Soc. Opt. Eng.* **1997**, *3105*, 96–103.

[53] K. Rurack, J. L. Bricks, B. Schulz, M. Maus, G. Reck, U. Resch-Genger, *J. Phys. Chem. A* **2000**, *104*, 6171–6188.

Received: February 26, 2006

